Kinetics of the Homopolymerization of Vinylidene Fluoride and Its Copolymerization with Hexafluoropropylene in Supercritical Carbon Dioxide: The Locus of Polymerization

Tamer S. Ahmed,[†] Joseph M. DeSimone,[†,‡] and George W. Roberts*[,†]

Department of Chemical and Biomolecular Engineering, North Carolina State University, Box # 7905, Raleigh, North Carolina 27695-7905, and Department of Chemistry, University of North Carolina at Chapel Hill, Box # 3290, Chapel Hill, North Carolina 27599-3290

Received August 22, 2008; Revised Manuscript Received November 7, 2008

ABSTRACT: In previous studies, the continuous polymerization of vinylidene fluoride (VF2) and mixtures of VF2 with hexafluoropropylene (HFP) was carried out in supercritical carbon dioxide ($scCO_2$) using a continuous stirred-tank reactor (CSTR). Most of the polymerizations were heterogeneous; i.e., polymer particles precipitated during the reaction. However, some were homogeneous, especially at higher HFP concentrations. In this study, the data from the earlier experiments have been tested against three kinetic models to determine the primary locus of the heterogeneous polymerizations. The first model, the "solution polymerization" model, is based on the assumption that all of the polymerization reactions take place in the continuous, CO_2-rich phase, with no reaction in the polymer phase. In the second model, the "surface polymerization" model, chain initiation occurs in the continuous phase, while chain propagation and termination occur in a thin zone on the surface of the polymer particles. The third model, the "interior polymerization" model, is similar to the "surface polymerization" model, except that propagation and termination take place uniformly throughout the polymer particles. For all polymer compositions, the solution polymerization model is able to describe the experimental data for both the rate of polymerization and the number-average molecular weight quite well. On the other hand, both the surface and the interior polymerization models consistently fail to fit the experimental results. This analysis suggests that the CO_2-rich continuous phase is the main locus of polymerization in the precipitation polymerization of VF2 and VF2/HFP mixtures in $scCO_2$ over the current range of the experimental data.

Introduction

Considerable effort has been devoted since the early 1990s to find environmentally benign solvents and processes for fluoropolymer synthesis, particularly as a result of increased environmental regulations.[1,2] Fluoropolymers are typically manufactured commercially in aqueous suspension or/and emulsion polymerization systems.[3] Such processes require the use of large quantities of water. Moreover, many of the fluorinated surfactants typically employed in aqueous emulsion polymerizations, and sometimes in suspension polymerizations, are currently under scrutiny due to bioaccumulation and environmental persistence.[4,5] These issues have created an impetus for transition from the conventional fluoropolymer synthesis processes to alternatives that meet the requirements of emerging public and regulatory demands.[6]

Supercritical carbon dioxide ($scCO_2$) has been demonstrated to be a promising alternative reaction medium for polymerizations.[2,7−13] Advantages of CO_2 are its environmental compatibility, low viscosity, ease of separation from the polymeric product, inertness to chain transfer reactions, and the ease of tuning of its properties because of its accessible critical point. In addition, monomers that are difficult or even impossible to polymerize in an aqueous system, either because of their solubility or because of their reaction with water, can be polymerized in $scCO_2$. Moreover, polymers produced in CO_2 show some unique physical or structural properties, which may facilitate processing or open new applications for such polymers.[14,15]

Only amorphous or low-melting fluoropolymers and silicones show appreciable solubility in $scCO_2$ at relatively mild temperatures and pressures ($T < 100$ °C, $P < 400$ bar).[1,16] These two classes of polymers can be synthesized by a homogeneous polymerization in $scCO_2$. However, polymers that are insoluble in $scCO_2$ under reasonable conditions must be made by heterogeneous methods, such as precipitation, dispersion, emulsion, and suspension polymerization. The majority of the polymerizations in $scCO_2$ reported in the literature are precipitation polymerizations and, to a lesser extent, dispersion polymerizations.[11]

During precipitation polymerization, polymer particles precipitate from the continuous phase. Depending on the characteristic time for polymerization compared to those for precipitation and transport of the macroradicals to the polymer particles, the growing radicals can either terminate in the continuous phase or enter the polymer phase without termination. In the latter case, propagation can continue in the polymer particles if there is an appreciable concentration of monomer(s) dissolved in the polymer phase. The partitioning of the monomer(s) between the polymer particles and the CO_2-rich fluid depends on many factors including the equilibrium solubility of the monomers in the polymer, hydrodynamic conditions in the reactor, and the size of the particles. Biomolecular termination reactions between macroradicals in the particles are very slow, since diffusion of the macroradicals and their chain ends is hindered in the polymer phase.

Accordingly, three limiting kinetic scenarios can be distinguished. First, initiation, propagation, and termination occur predominantly in the continuous phase. This scenario results if the kinetics of termination in the fluid is much faster than the kinetics of precipitation and/or transport of macroradicals into the polymer phase. A similar situation occurs if the solubility of the monomer(s) in the polymer is so low that propagation in the polymer phase is very slow. The second scenario is when the radicals grow in the fluid phase until precipitation/transport

* To whom correspondence should be addressed: Tel +1-919-515-7328; Fax +1-919-515-3465; e-mail groberts@eos.ncsu.edu.
[†] North Carolina State University.
[‡] University of North Carolina at Chapel Hill.

10.1021/ma801911j CCC: $40.75
Published on Web 12/16/2008

takes place, and then the radicals continue growing in the polymer phase. In this case, both phases can be important loci of polymerization. The third scenario occurs when the growing radicals precipitate at very low chain lengths and polymerization continues in the polymer phase. In that case, the polymer phase is the main locus of polymerization.

The question of where polymerization occurs is of both theoretical interest and practical importance. An improperly controlled reaction can give rise to operational difficulty and safety problems and can lead to out-of-specification product. In addition, knowledge of the locus of polymerization can help in tailoring the polymer properties. For example, the precipitation polymerization of poly(acrylic acid) (PAA) in $scCO_2$ appears to occur predominantly in the polymer phase.[17] Consequently, it was possible to synthesize cross-linked PAA particles in a single-step, continuous process simply by adding a multifunctional monomer (cross-linker) to the monomer that was fed to the reactor.[18] By varying the cross-linker concentration, the polymer product could be made soluble, partially soluble, or insoluble in water. If polymerization had occurred primarily in the fluid phase, adding a cross-linker to the feed might have resulted in a solid mass of polymer that filled the reactor.

Two methodologies have been developed to aid in determining the locus of a given precipitation polymerization. The first is by Mueller et al.,[19] who developed a mathematical model for the precipitation polymerization process that can be used to predict the relative contributions of the two different loci to the overall polymerization. This approach can be predictive if all of the parameters in the model are known a priori. However, the model contains a large number of parameters, and many of them can be difficult to obtain or estimate. Not unexpectedly, the results of the analysis are very dependent on the accuracy of several of these parameters. This model was applied to the dispersion polymerization of poly(methyl methacrylate) (PMMA) in $scCO_2$[19,20] and to the precipitation polymerization of poly(vinylidene fluoride) (PVDF) in $scCO_2$.[21] The application to PMMA was completely predictive. However, in the case of PVDF, three parameters were used as adjustable parameters to fit the experimental data, although the exact fitting was not discussed.[21]

The second methodology to determine the main locus of polymerization requires experimental data taken in a continuous stirred-tank reactor (CSTR).[17] Briefly, a set of steady-state experiments are carried out, such that the amount of polymer in the reactor is varied at constant temperature and reaction pressure. This can be accomplished by changing the inlet monomer concentration, and/or the inlet initiator concentration, and/or the average residence time at constant temperature and pressure. The variation of the rate of polymerization (R_P) and number-average molecular weight (M_n) with the polymer volume fraction in the CSTR permits one to distinguish between polymerization in the continuous phase, on the surface of the precipitated polymer particles, or inside the particles. This methodology was applied to the precipitation polymerization in $scCO_2$ of PAA by Liu et al.[17] and suggested that the main locus of polymerization was the polymer phase. This approach is nonpredictive since it requires experimental data from a CSTR.

Vinylidene fluoride (VF2) homopolymer and copolymers with hexafluoropropylene (HFP) are important commercial fluoropolymers.[3] The homopolymer (PVDF) is used in applications requiring the highest purity, strength, and resistance to solvents, acids, bases, and heat, in addition to low smoke generation during a fire. It is widely used for fabricating pipe, tubing, column packing, valves, pumps, and membranes.[22] Vinylidene fluoride copolymers with HFP are divided into two main categories: (a) the low-HFP-content, semicrystalline copolymers containing about 5−15 mol % HFP and (b) the high-HFP-content, amorphous copolymers with HFP higher than 19−20 mol %.[23−26] The low-HFP-content copolymers are used in tubing, valves and fittings, cable and wire jacketing, lithium-ion batteries, and membranes, while the high-HFP-content copolymers are used mainly as polymer processing aids to improve extrusion, blow molding, and rotomolding, and in sealing such as in gaskets and O-rings.

Telomers of VF2 are soluble in $scCO_2$ under 300 bar[27] while the high-molecular-weight homopolymer is only soluble above 1500−1700 bar and 130−140 °C.[28,29] On the contrary, VF2/HFP copolymers with high HFP content are soluble in $scCO_2$ at much milder conditions.[24,28,30] Therefore, precipitation or dispersion polymerizations are the predominant ways of polymerization of VF2 in $scCO_2$. Both batch[9,16,21,31−35] and continuous polymerization[15,36−38] were reported. Copolymerization of VF2 with HFP has been studied mostly in batch reactors.[30,39,40] The only exception is the continuous precipitation polymerization of low-HFP-content, semicrystalline poly(VF2-*co*-HFP)[23] and the continuous precipitation and solution polymerizations of the high-HFP-content, amorphous poly(VF2-*co*-HFP)[24] in $scCO_2$.

Bimodal molecular weight distributions (MWDs) were observed during the homopolymerization of VF2 in $scCO_2$,[21,38] especially at high monomer concentrations. There was only a long tail/shoulder for low-HFP-content copolymers, depending on the monomer concentration.[23] For high-HFP-content copolymers, a tail was observed only for very high monomer concentrations, for a copolymer composition of about 23 mol % HFP.[24] When the HFP content was about 26 mol % HFP and higher, there was no tail, and the MWDs were perfectly unimodal with a polydispersity index (PDI) of 1.5.[24]

The bimodality and broad MWD of PVDF is the subject of some controversy. The bimodality has been attributed either to a simultaneous polymerization in both the fluid and the polymer phases, taking into account the transport of polymeric radicals between the two phases,[21] or to a homogeneous polymerization, recognizing the transition of the termination reaction from a kinetically controlled regime to a diffusion-controlled regime with increasing macroradical molecular weight.[41]

In this publication, the methodology reported by Liu et al.[17] is applied to the precipitation homopolymerization of VF2 and to the precipitation and homogeneous copolymerization of VF2 with HFP in $scCO_2$. The results of this analysis help to resolve the controversy concerning the locus of polymerization, help to understand how the polymerization of these fluoromonomers proceeds in $scCO_2$, and help to identify the source of the bimodality of PVDF and the tail/shoulder of VF2/HFP copolymers.

Experimental Section

All of the data used in the present analysis have been reported previously. The experimental equipment and procedures are described in a series of publications.[23,24,36−38,42] A CSTR was used for all the experiments. The continuous polymerization of VF2 in $scCO_2$ was carried out at 276 bar and 75 °C with diethylperoxydicarbonate (DEPDC) as the free radical initiator.[36−38,42] For the low-HFP-content poly(VF2-*co*-HFP) (containing ca. 9.2 mol % HFP), the copolymerization was done at 400 bar and 40 °C using perfluorobutyryl peroxide (PBP) as the free radical initiator.[23] Finally, the synthesis of high-HFP-content poly(VF2-*co*-HFP) was reported recently.[24] Three different copolymer compositions (ca. 23.3, 26.3, and 30.3 mol % HFP) were studied at 400 bar and 40 °C using PBP initiator. Some reactions were heterogeneous (i.e., polymer precipitated during the reaction), and some were homogeneous (solution) polymerizations. The mode of polymerization depended on the copolymer composition and molecular weight. The experimental results that are analyzed below for the continuous

precipitation polymerization of PVDF were reported by Saraf et al.[38] They were generated at constant temperature and pressure by changing either the inlet monomer concentration (VF2/$scCO_2$ weight ratio: 0.057−0.24) or the average residence time at either low or high inlet monomer concentrations to the CSTR. The steady-state fractional conversions of monomer were 16−18.5% for data generated from the change of inlet monomer concentration and 11−27% and 9−21% for data generated from changing the average residence time at low and high inlet monomer concentrations, respectively. The results for low-and high-HFP-content poly(VF2-*co*-HFP)[23,24] were generated at constant temperature and pressure by changing the inlet monomer concentration (VF2/$scCO_2$ weight ratio: 0.23−1.38, 0.23−2.2, 0.24−2.35, and 0.25−2.6 for the 27/73, 59/41, 66/34, and 73/27 HFP/VF2 molar feed ratios corresponding to 9.2, 23.3, 26.3, and 30.3 mol % HFP copolymers, respectively). The steady-state conversions ranged from 8% to 9.5%.

Results and Discussion

Precipitation polymerization can occur at three different loci: the continuous solution phase, the surface of the precipitated polymer particles, or the interior of the precipitated polymer particles. The relative importance of these loci may depend on the reaction conditions. To understand the physical mechanism and kinetics of PVDF and poly(VF2-*co*-HFP) precipitation polymerization, three mathematical models that correspond to these three polymerization loci are compared with the experimental results.

Solution Polymerization Model. The main characteristic of the solution polymerization model is that all the reactions (initiation, propagation, and termination) occur in the continuous phase, with no reaction in the polymer phase. This implies that the characteristic time of termination of radicals in the fluid phase is much less than that for their precipitation and/or transport to the polymer particles, so that the polymeric radicals grow and terminate in the fluid before precipitation and/or transport to the solid polymer particles. Alternatively, the solution polymerization model may apply if the solubility of the monomer(s) in the polymer is very low, so that the rate of propagation in the solid phase is small compared to that in the fluid. This scenario is one limiting case of the reaction behavior.

Liu et al.[17] derived eqs 1 and 2 for the volumetric rate of polymerization (R_P) and the number-average molecular weight (M_n) for solution polymerization in a CSTR at steady state, in the presence of polymer particles. The volume fraction of particles is designated (υ_p) and is given by eq 3. As υ_p approaches zero, the expressions for R_P and M_n (eqs 1 and 2) reduce to the classical expressions for solution polymerization.[43]

$$R_P = k_p\left(\frac{2fk_d}{2k_t}\right)^{0.5}\frac{[M_T]_{out}[I]_{out}^{0.5}(1-\upsilon_p)}{[1+(\alpha-1)\upsilon_p][1+(\beta-1)\upsilon_p]^{0.5}} \quad (1)$$

$$\frac{M_n}{M_o} = \frac{\psi k_p}{(2fk_d(2k_t))^{0.5}}\frac{[M_T]_{out}[I]_{out}^{-0.5}[1+(\beta-1)\upsilon_p]^{0.5}}{1+(\alpha-1)\upsilon_p} \quad (2)$$

$$\upsilon_p = \frac{x[M_T]_{in}M_o}{\rho_p} \quad (3)$$

Here k_p and $2k_t$ are the average propagation and termination rate constants for the copolymerization; k_d and f are the initiator decomposition rate constant and decomposition efficiency; $[M_T]_{out}$ and $[I]_{out}$ are the concentrations of total monomer and initiator in the CSTR and in the effluent from the CSTR; R_P is the total volumetric rate of polymerization; α and β are the equilibrium partition coefficients of the total monomer and initiator between the polymer phase and the continuous phase (i.e., the ratio of the concentration in the polymer phase to that in the continuous phase); ψ equals 1 or 2 for termination by disproportionation or combination, respectively; M_o is the average molecular weight of a monomer unit in the polymer; x is the steady-state conversion in the CSTR; $[M_T]_{in}$ is the total monomer concentration in the feed to the CSTR; ρ_p is the polymer density. Equations 1 and 2 are based on the assumption that both monomer and initiator are in equilibrium between the fluid and polymer phases and that the partition coefficients (α, β) do not depend on either concentration.

The original expressions derived by Liu et al. were for homopolymerization. However, with some modifications, they can be applied to copolymerization. For example, at constant temperature and pressure, the copolymerization propagation rate constant (k_p) is a function of the mole fractions of the monomers and their reactivity ratios. Equation 4 shows the expression for k_p in the case of the terminal model.[43] In addition, the copolymerization termination rate constant is a combination of the termination rate constants for the two homopolymerizations. The termination rate is usually diffusion-controlled,[43,44] and the simplest "ideal diffusion" model for k_t is given by a linear combination of the termination rate constants for the two homopolymerizations (eq 5).[45]

$$k_p = \frac{r_1f_1^2 + 2f_1f_2 + r_2f_2^2}{(r_1f_1/k_{11}) + (r_2f_2/k_{22})} \quad (4)$$

$$k_t = F_1k_{t1} + F_2k_{t2} \quad (5)$$

In these equations f_i, F_i, r_i, k_{ii}, and k_{ti} are the mole fraction in the feed, mole fraction in the copolymer, reactivity ratio, homo-propagation rate constant, and homo-termination rate constant for monomer *i,* respectively.

The values of k_p and k_t, given by eqs 4 and 5, depend on the composition of the fluid phase (f_1, f_2) and the composition of the copolymer (F_1, F_2). For each of the five polymer compositions studied, these mole fractions were nearly constant, although they varied from one composition to another. Therefore, it is reasonable to expect that k_p and k_t were essentially constant for each composition.

Equation 1 can be rearranged to give eq 6. If α and β both are zero, the right-hand side of eq 6 will be a constant that depends on temperature and pressure but is independent of υ_p. In this case, all of the monomer(s) and initiator are in the continuous phase; i.e., there is no partitioning of these components into the polymer particles. If α and/or β are greater than zero, the right-hand side of eq 6 decreases with increasing υ_p since some of the monomer(s) and/or initiator are "stored" in the polymer particles, where they do not participate in the polymerization according to the assumption of the solution polymerization model. Consequently, an increase in $R_P(1-\upsilon_p)^{0.5}/([M_T]_{out}[I]_{out}^{0.5})$ as υ_p increases is a clear indication that the solution polymerization model is not obeyed.

$$\frac{R_P(1-\upsilon_p)^{0.5}}{[M_T]_{out}[I]_{out}^{0.5}} = k_p\left(\frac{2fk_d}{2k_t}\right)^{0.5}\frac{(1-\upsilon_p)^{1.5}}{[1+(\alpha-1)\upsilon_p][1+(\beta-1)\upsilon_p]^{0.5}} \quad (6)$$

$$\frac{M_n[I]_{out}^{0.5}(1-\upsilon_p)^{0.5}}{M_o[M_T]_{out}} = \frac{\psi k_p}{(2fk_d(2k_t))^{0.5}}\frac{[1+(\beta-1)\upsilon_p]^{0.5}(1-\upsilon_p)^{0.5}}{1+(\alpha-1)\upsilon_p} \quad (7)$$

Similarly, eq 2 can be rearranged to give eq 7. The effect of monomer(s) and initiator partitioning on M_n is more complex than in case of R_P. If α and β both are zero, the right-hand side

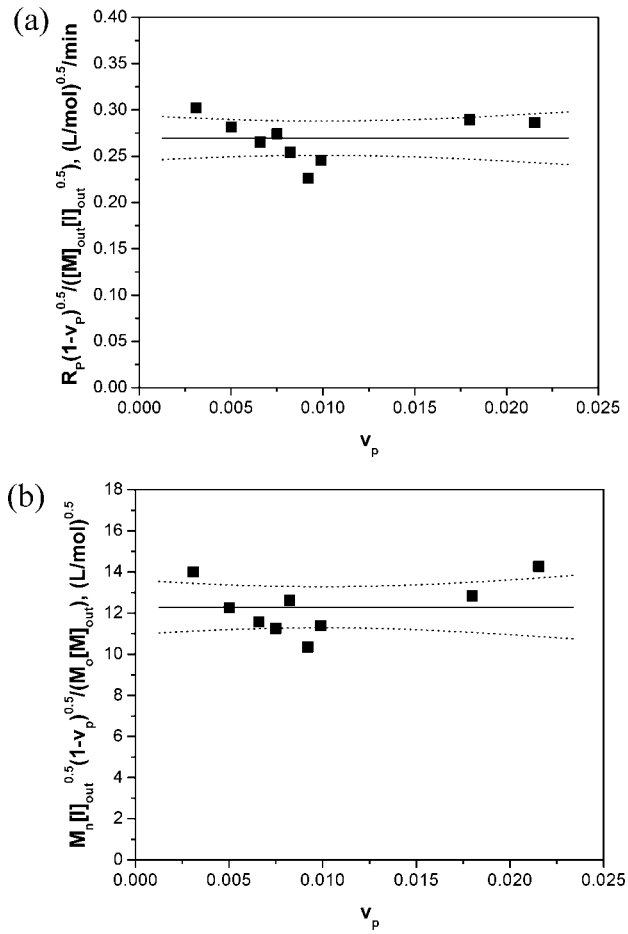

Figure 1. Test of the solution polymerization model for polymerization of PVDF in a CSTR: (a) rate of polymerization, (b) molecular weight; $P = 276$ bar, $T = 75$ °C, varying inlet monomer concentration and average residence time.[38] The line is the best horizontal linear fit for the data. The dotted points are the 95% confidence bands for the linear fit.

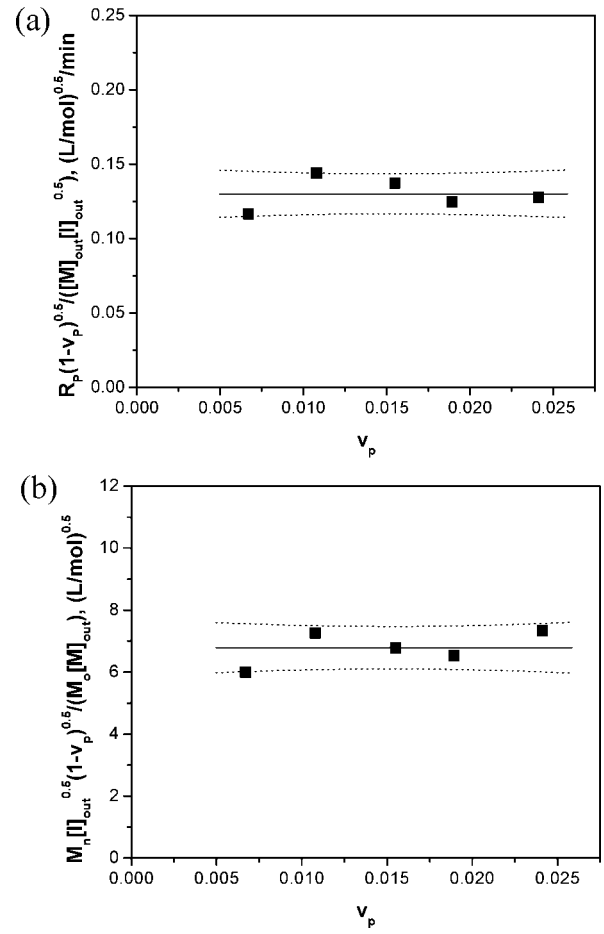

Figure 2. Test of the solution polymerization model for the polymerization of low-HFP-content poly(VF2-*co*-9.2 mol % HFP) in a CSTR: (a) rate of polymerization, (b) molecular weight; $P = 400$ bar, $T = 40$ °C, varying inlet monomer concentration.[23] The line is the best horizontal linear fit for the data. The dotted points are the 95% confidence bands for the linear fit.

of eq 7 will be independent of v_p but will depend on temperature and pressure. For any other values for α and/or β, the right-hand side of eq 7 will decrease with v_p unless β is high enough to outweigh the effect of α. In this case, the decrease of the initiator concentration in the continuous phase with increasing v_p has a greater effect than the decrease of the monomer(s) concentration(s), causing the right-hand side to increase and resulting in higher molecular weight polymers. In any event, unless α and/or β are very large compared to unity, the left-hand sides of eqs 6 and 7 are relatively weak functions of v_p.

Tests of the experimental data against the solution polymerization model are shown in Figures 1, 2, and 3 for PVDF, low-HFP-content poly(VF2-*co*-HFP), and high-HFP-content poly(VF2-*co*-HFP), respectively. The experimental data for PVDF were generated by varying the inlet monomer concentration and the residence time at 75 °C and 276 bar.[38] The maximum value of v_p in these experiments is about 0.022. Significantly higher values for v_p could not be achieved during the continuous experiments for several reasons. First, at very high initial monomer concentrations, the monomer is not completely soluble in $scCO_2$. Second, high values of inlet monomer concentration or average residence time resulted in instability in the operation of the CSTR; i.e., steady state could not be reached.[38] This instability was attributed to the occurrence of gelation at these conditions.[38] Somewhat higher values of v_p were achieved in batch polymerizations.[21] However, these values represent the cumulative amount of polymer at the end of the batch reaction. There is one reported batch experiment with an initial VF2 concentration of 6.2 M, a final conversion of about 25%, and a final v_p of 0.056.[21] However, this experiment might have exhibited instabilities similar to those observed in the CSTR at similar conditions.[46] Significantly, the data that are analyzed herein include the conditions at which the bimodal MWDs of PVDF were observed. Specifically, bimodality was observed at values of v_p between 0.01 and 0.022 in the CSTR experiments. For the batch experiments, bimodality was observed at final v_p values higher than 0.008.

The experimental data for the low- and high-HFP-content poly(VF2-*co*-HFP) were generated by changing the inlet total monomer concentration up to 6.5 M at 40 °C and 400 bar.[23,24] For the copolymers, values of v_p were somewhat higher than for PVDF since it was possible to use much higher total monomer feed concentrations.

Parts a and b of Figure 1 show plots of $R_P(1 - v_p)^{0.5}/([M_T]_{out}[I]_{out}^{0.5})$ and $M_n[I]_{out}^{0.5}(1 - v_p)^{0.5}/(M_o[M_T]_{out})$ vs v_p, respectively, for PVDF. Overall, both of these parameters are essentially independent of v_p. However, both show a slightly decreasing trend with increasing v_p at low values of v_p. This decrease is consistent with some partitioning of monomer and/or initiator into the polymer particles. The decreases in $R_P(1 - v_p)^{0.5}/([M_T]_{out}[I]_{out}^{0.5})$ and $M_n[I]_{out}^{0.5}(1 - v_p)^{0.5}/(M_o[M_T]_{out})$ do not continue for the two highest polymer volume fractions. Gelled fractions of PVDF are known to occur at high monomer concentrations (high v_p) as a result of termination by combination coupled with chain transfer to polymer.[47] It may be that

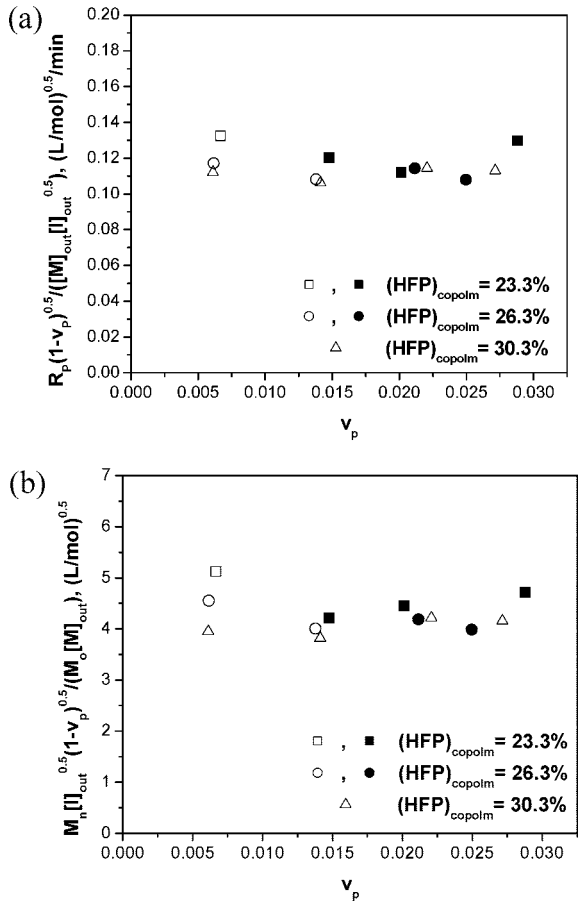

Figure 3. Test of the solution polymerization model for the polymerization of high-HFP-content poly(VF2-*co*-HFP) in a CSTR: (a) rate of polymerization, (b) molecular weight; $P = 400$ bar, $T = 40$ °C, varying inlet monomer concentration.[24] Filled symbols: precipitation polymerization; open symbols: homogeneous polymerization. For homogeneous polymerization, v_p should be zero. Open points shown in figure are for hypothetical values using eq 3 and assuming that the polymer precipitated.

the presence of these gels reduces the values of α and/or β somewhat relative to their values in the ungelled polymer. Nevertheless, the data in both Figure 1a,b are quite consistent with the solution polymerization model and suggest that the continuous phase was the primary locus of polymerization for these PVDF experiments.

Parts a and b of Figure 2 show plots of $R_P(1 - v_p)^{0.5}/([M_T]_{out}[I]_{out}^{0.5})$ and $M_n[I]_{out}^{0.5}(1 - v_p)^{0.5}/(M_o[M_T]_{out})$ vs v_p, respectively, for low-HFP-content poly(VF2-*co*-HFP). Both parameters in Figure 2 are essentially constant. This behavior is also consistent with the solution polymerization model, for conditions where the partitioning of the monomers and initiator is relatively small.

Finally, Figures 3a,b test the solution polymerization model against the data for the high-HFP-content poly(VF2-*co*-HFP). Three different copolymers are shown, with HFP contents of 23.3, 26.3, and 30.3 mol %. The filled symbols in Figure 3 are for experiments where the polymer precipitated; i.e., polymer particles were present in the reactor at steady state. The open symbols are for homogeneous polymerizations, where no precipitation occurred. For both the 23 and the 26 mol % HFP copolymers, the mode of polymerization (i.e., precipitation or homogeneous) had no effect on the trend of the experimental data. The values of $R_P(1 - v_p)^{0.5}/([M_T]_{out}[I]_{out}^{0.5})$ and $M_n[I]_{out}^{0.5}(1 - v_p)^{0.5}/(M_o[M_T]_{out})$ are essentially the same whether or not polymer was present in the reactor. All of the data for each copolymer composition fall on essentially the same horizontal straight line. This confirms that the polymer phase does not make a significant contribution to the polymerization kinetics. The data for all the three high-HFP-content copolymers are very consistent with the solution polymerization model.

Note that all of the polymerizations were homogeneous for the 30.3% HFP copolymer. The fact that the solution polymerization model describes the data for this composition essentially perfectly lends confidence to the physical and mathematical foundation of this model and its use to interpret the behavior of heterogeneous polymerizations.

Surface Polymerization Model. This model is based on two main assumptions. First, growing polymer chains precipitate or transport to the polymer phase at very low chain lengths, so that the rate of polymerization in the continuous fluid phase is negligible compared to that in the polymer phase. This assumption implies that the characteristic time of termination in the fluid phase is very long compared to that for transfer of radicals to the polymer phase via precipitation and/or transport. Second, diffusion of monomer(s) into the polymer particles is slow relative to the propagation reaction, so polymerization takes place primarily in a thin layer on the particle surface. Chain initiation is assumed to take place in the solution phase, but chain propagation and chain termination take place exclusively on the polymer particle surface. Initiation in the polymer phase is ignored. This assumption can be rationalized by the expected low decomposition efficiency of the initiator in the polymer particles since the efficiency is usually diffusion-controlled.[43] As with the solution polymerization model, phase equilibrium is assumed for monomer and initiator, and the partition coefficients are assumed to be independent of concentration.

The overall rate of polymerization and the number-average molecular weight for the surface polymerization model are given by eqs 8 and 9 for polymerization in an ideal CSTR.[17] If the surface polymerization model is obeyed, plots of $R_P/([M_T]_{out}[I]_{out}^{0.5})$ and $M_n[I]_{out}^{0.5}/M_0[M_T]_{out}$ vs the cubic root of the volume fraction of the polymer in the reactor must form a straight line passing through the origin for constant temperature, pressure, reaction zone thickness (δ), and number of polymer particles per unit volume of the reactor (N). The value of δ is determined by the balance between monomer(s) diffusivity and the rate of the propagation reaction, which in turn depends on temperature and pressure but should be essentially independent of v_p. Usually N depends on the rate of initiation, which is a function of temperature, pressure, initiator concentration in the feed, and the average residence time in the CSTR. However, the dependence of eqs 8 and 9 on N is rather weak since it is raised to the 1/6 power. Thus, the right-hand side of eqs 8 and 9 should depend on $v_p^{1/3}$, plus temperature and pressure.

$$\frac{R_P}{[M_T]_{out}[I]_{out}^{0.5}} = (36\pi N)^{1/6}\alpha\delta^{0.5}k_p\left(\frac{2fk_d}{2k_t}\right)^{0.5}v_p^{1/3} \quad (8)$$

$$\frac{M_n[I]_{out}^{0.5}}{M_o[M_T]_{out}} = \frac{\psi(36\pi N)^{1/6}\alpha\delta^{0.5}k_p}{(2fk_d(2k_t))^{0.5}}v_p^{1/3} \quad (9)$$

The surface polymerization model is distinguished from the solution polymerization model by a different dependence of both the R_P and M_n on v_p. The dependence of the R_P and M_n in the case of the surface polymerization model is much stronger than in case of the solution polymerization model (essentially independent of v_p). If the surface polymerization model is obeyed, $R_P/([M_T]_{out}[I]_{out}^{0.5})$ and $M_n[I]_{out}^{0.5}/(M_o[M_T]_{out})$ should depend on $v_p^{1/3}$. Clearly, the previous tests of the solution polymerization model show that the data for the three polymer systems will not agree with the surface polymerization model.

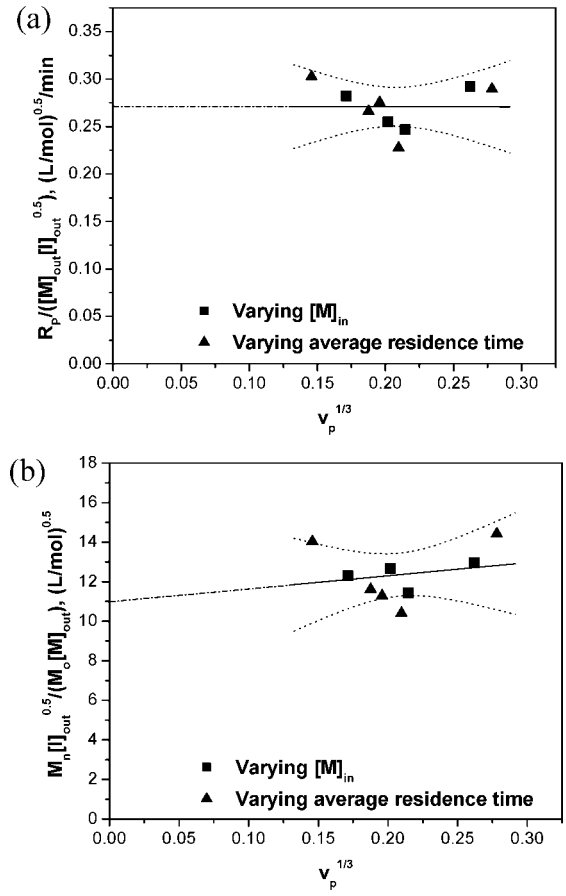

Figure 4. Test of the surface polymerization model for the polymerization of PVDF in a CSTR: (a) rate of polymerization, (b) molecular weight; $P = 276$ bar, $T = 75$ °C, varying inlet monomer concentration and average residence time.[38] The line is the best linear fit for the data allowing for a nonzero intercept. The dotted points are the 95% confidence bands for the linear fit.

Nevertheless, for completeness, the data for PVDF are tested against this model below. Tests for the copolymer systems are provided in the Supporting Information.

The test of the surface polymerization model for PVDF precipitation polymerization is shown in parts a and b of Figure 4 for the R_P and M_n data, respectively. All the data for PVDF were used in the test of the surface polymerization model. However, for the sake of accuracy, the experimental data in Figures 4a,b generated by varying the average residence time are distinguished from those generated by varying the inlet monomer concentration since N can be affected by the average residence time.

In fitting the data in Figure 4a,b, the straight line was not forced through the origin, as the surface polymerization model requires. Clearly, a straight line through the origin would not fit either set of data. Allowing a nonzero intercept tests the possibility that a portion of polymerization was homogeneous and a portion took place on the surface of the polymer particles. The intercept on the y-axis obtained from such a fit is the value of $R_P/([M_T]_{out}[I]_{out}^{0.5})$ or $M_n[I]_{out}^{0.5}/(M_o[M_T]_{out})$ that results from polymerization in the fluid phase, i.e., at $v_p = 0$. A positive slope then would indicate the contribution of surface polymerization.

Obviously, there is essentially no contribution from surface polymerization to the R_P data as shown in Figure 4a. As for the M_n data, the slight positive slope in Figure 4b appears to suggest that surface polymerization makes some small contribution to molecular-weight development. However, the difference between the intercept and the average of the data is not statistically significant at the 95% confidence level. In addition, the slope itself is not statistically different from zero at the same level. Clearly, the surface polymerization model is not obeyed. Moreover, the lack of any statistically significant dependence of either $R_P/([M_T]_{out}[I]_{out}^{0.5})$ or $M_n[I]_{out}^{0.5}/(M_o[M_T]_{out})$ on $v_p^{1/3}$ suggests that surface polymerization does not contribute measurably to either the rate of polymerization or to molecular-weight development, at the conditions of these experiments.

Interior Polymerization Model. The interior polymerization model shares several important features with the surface polymerization model. First, the rate of polymerization in the continuous phase is negligible compared to that in the polymer phase. In addition, initiation takes place exclusively in the fluid phase, and phase equilibrium is assumed for both monomer and initiator. The two models differ in the way in which the monomer distributes throughout the polymer particles. In the interior polymerization model, the polymerization is assumed to occur homogenously throughout the whole volume of the particles and is not restricted to a thin layer on the particle surface. With these assumptions, R_P and M_n for the copolymerization are described by eqs 10 and 11 for polymerization in an ideal CSTR.[17]

$$\frac{R_P}{[M_T]_{out}[I]_{out}^{0.5}} = \alpha k_p \left(\frac{2fk_d}{2k_t}\right)^{0.5} v_p^{1/2} \tag{10}$$

$$\frac{M_n[I]_{out}^{0.5}}{M_o[M_T]_{out}} = \frac{\psi \alpha k_p}{(2fk_d(2k_t))^{0.5}} v_p^{1/2} \tag{11}$$

If the interior polymerization model is obeyed, both $R_P/([M_T]_{out}[I]_{out}^{0.5})$ and $M_n[I]_{out}^{0.5}/(M_o[M_T]_{out})$ will be linear functions of $v_p^{1/2}$ passing through the origin. Once again, the earlier analysis of the solution polymerization model establishes that the experimental data will not be described by the interior polymerization model. However, for completeness, the data for PVDF are tested below, while the tests for the copolymer systems are provided in the Supporting Information.

The test of the interior polymerization model for PVDF is shown in Figures 5a,b. The precipitation polymerization of PVDF cannot be described solely by this model. Although both "best fit" lines have a slight positive slope, the values of these slopes are once again not statistically different from zero. Therefore, as described in the previous section, interior polymerization does not contribute significantly to either the polymerization rate or the molecular weight development, at the conditions of these experiments.

The preceding analysis demonstrates that, for the data considered, the precipitation polymerizations of VF2 homopolymer and copolymers with HFP in $scCO_2$ occur in the continuous CO_2-rich phase, at the conditions of the experiments. As discussed earlier, this suggests that either termination in the fluid phase is much faster than precipitation and/or transport of macroradicals to the polymer phase or the solubility of VF2 in the polymer is very low. The simultaneous sorption of CO_2 and VF2 into PVDF was recently reported by Galia et al.,[48] who showed that the concentration of VF2 in the polymer particles is very low in the presence of $scCO_2$. These results are supported by a similar study by our research group.[15,49] These solubility studies suggest that any macroradical that may be initiated or captured in the polymer phase propagates under monomer-starved conditions that compensate for the autoacceleration effect arising from impeded termination in the polymer phase. Consequently, even if the macroradicals do precipitate or transport to the polymer particles before termination, their contribution to the overall polymerization will be small.

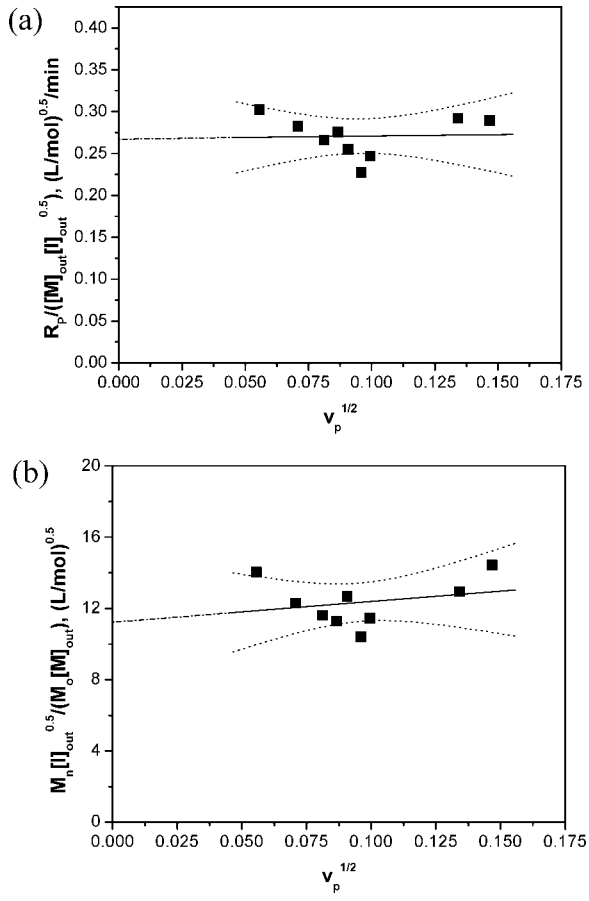

Figure 5. Test of the interior polymerization model for the polymerization of PVDF in a CSTR: (a) rate of polymerization, (b) molecular weight; $P = 276$ bar, $T = 75$ °C, varying inlet monomer concentration and average residence time.[38] The line is the best linear fit for the data allowing for a nonzero intercept. The dotted points are the 95% confidence bands for the linear fit.

Considering the continuous phase as the main locus of polymerization can help in understanding some features of VF2 polymerization. For example, during one of the experiments on the precipitation polymerization of PVDF in our laboratory, a tough, essentially insoluble, polymer that filled the whole reactor was produced.[38,50] It has been suggested that chain transfer to polymer occurs for VF2 polymers.[47] Moreover, termination is by combination.[38] This mechanism of cross-linking can produce the tough polymer that filled the reactor, provided that polymerization took place primarily in the fluid phase. If polymerization occurred mainly in the polymer phase, only cross-linked polymer particles would have been produced, similar to the result with PAA.[18] Moreover, it has been suggested that the bimodal MWD that has been observed for PVDF is the result of simultaneous polymerization in the two phases. The low molecular weight peak was attributed to polymerization in the CO_2-rich phase, while the high molecular weight peak was attributed to polymerization in the polymer particles.[21] Clearly, this is not the case for the present experimental data. An approximate deconvolution of the data of Saraf et al.[38] for the PVDF experiments at 2.8 and 3.5 mol/L VF2 inlet concentrations shows that approximately 60−70% of the monomer units are in the second, high-molecular-weight peak. Attributing this peak to polymerization in the polymer particles is clearly incompatible with the excellent fit of the data to the solution polymerization model and to the lack of fit to the surface and interior polymerization models. It is also inconsistent with the very low solubility of VF2 in PVDF in presence of CO_2.[15,48,49] Additional features of the copolymerization of VF2 and HFP that can be accounted for by recognizing that the continuous, CO_2-rich phase is the main locus of polymerization were discussed in our recent contributions.[23,24]

Finally, it is must be recognized that the models developed by Liu et al. depend on the assumptions used in their derivations.[17] These models do not contain many complexities of the polymerization chemistry and physics: details of phase behavior, particle formation, interphase mass transfer, etc. Nevertheless, these models do capture the difference in kinetic behavior between the two major loci of polymerization, the fluid phase and the polymer particles. Therefore, as demonstrated here, these models are very useful tools for the analysis of data obtained in a CSTR to distinguish between the possible loci of polymerization. It is interesting to note the difference in behavior between the "CO_2-phobic" PAA polymerization[17] and the "CO_2-philic" VF2 homo- and co- polymerization with HFP.

Conclusions

The experimental data for the polymerization of VF2 and VF2/HFP mixtures in $scCO_2$ in a CSTR have been tested against three different kinetic models that assume different loci of polymerization. In the solution polymerization model, the polymerization reactions occur only in the fluid phase, with no reactions in the polymer phase. For the surface and interior polymerization models, chain initiation takes place in the fluid phase, but chain propagation and termination occur either on the polymer surface (surface polymerization model) or homogeneously throughout the polymer particle (interior polymerization model).

The solution polymerization model accounts quite well for the observed behavior of both the rate of polymerization and the number-average molecular weight for PVDF and poly(VF2-*co*-HFP). On the other hand, the two models based on polymerization in the polymer phase are unable to fit the experimental data. Moreover, for the same copolymer composition, the kinetic behavior of homogeneous VF2/HFP polymerizations was the same as that of heterogeneous (precipitation) polymerizations. This analysis demonstrates that the continuous CO_2-rich phase is the main locus of polymerization for the precipitation polymerization of VF2 homo- and copolymers with HFP in $scCO_2$, at the conditions studied.

Acknowledgment. This material is based upon work supported by the STC Program of the National Science Foundation under Agreement CHE-9876674.

Supporting Information Available: Tests of the surface and interior polymerization models against the low- and high-HFP-content polymerization data. This material is available free of charge via the Internet at http://pubs.acs.org.

References and Notes

(1) DeSimone, J. M.; Tumas, W. *Green Chemistry Using Liquid and Supercritical Carbon Dioxide*; Oxford University Press: New York, 2003.
(2) DeSimone, J. M. *Science* **2002**, *297* (5582), 799–803.
(3) Scheirs, J. *Modern Fluoropolymers: High Performance Polymers for Diverse Applications*; John Wiley & Sons: New York, 1997.
(4) Preliminary Risk Assessment: Perfluorooctanic Acid (PFOA) and Fluorinated Telomers; US Environmental Protection Agency, April 2003.
(5) 2010/15 PFOA Stewardship Program; U.S. Environmental Protection Agency. Jan 2006.
(6) Wood, C. D.; Cooper, A. I.; DeSimone, J. M. *Curr. Opin. Solid State Mater. Sci.* **2004**, *8* (5), 325–331.
(7) Cooper, A. I. *J. Mater. Chem.* **2000**, *10* (2), 207–234.
(8) Canelas, D. A.; DeSimone, J. M. *Adv. Polym. Sci.* **1997**, *133*, 103–140.
(9) Kendall, J. L.; Canelas, D. A.; Young, J. L.; DeSimone, J. M. *Chem. Rev.* **1999**, *99* (2), 543–563.

(10) Ajzenberg, N.; Trabelsi, F.; Recasens, F. *Chem. Eng. Technol.* **2000**, *23* (10), 829–839.
(11) Beckman, E. J. *J. Supercrit. Fluids* **2004**, *28* (2−3), 121–191.
(12) Kennedy, K. A.; Roberts, G. W.; DeSimone, J. M. *Adv. Polym. Sci.* **2005**, *175*, 329–346.
(13) Kemmere, M. F.; Meyer, T. *Supercritical Carbon Dioxide in Polymer Reaction Engineering*; Wiley-VCH: Weinheim, 2005.
(14) Liu, T.; Garner, P.; DeSimone, J. M.; Roberts, G. W.; Bothun, G. D. *Macromolecules* **2006**, *39* (19), 6489–6494.
(15) Saraf, M. K.; Wojcinski, L. M., II.; Kennedy, K. A.; Gerard, S.; Charpentier, P. A.; DeSimone, J. M.; Roberts, G. W. *Macromol. Symp.* **2002**, *182*, 119–129.
(16) DeSimone, J. M.; Maury, E. E.; Menceloglu, Y. Z.; McClain, J. B.; Romack, T. J.; Combes, J. R. *Science* **1994**, *265* (5170), 356–359.
(17) Liu, T.; DeSimone, J. M.; Roberts, G. W. *Chem. Eng. Sci.* **2006**, *61* (10), 3129–3139.
(18) Liu, T.; DeSimone, J. M.; Roberts, G. W. *Polymer* **2006**, *47* (12), 4276–4281.
(19) Mueller, P. A.; Storti, G.; Morbidelli, M. *Chem. Eng. Sci.* **2004**, *60* (2), 377–397.
(20) Mueller, P. A.; Storti, G.; Morbidelli, M. *Chem. Eng. Sci.* **2005**, *60* (7), 1911–1925.
(21) Mueller, P. A.; Storti, G.; Apostolo, M.; Martin, R.; Morbidelli, M. *Macromolecules* **2005**, *38* (16), 7150–7163.
(22) Dohany, J. E. Poly(Vinylidene Fluoride). In *Kirk-Othmer Encyclopedia of Chemical Technology*, 4th ed.; Kirk-Othmer, Ed.; John Wiley & Sons: New York, 1998.
(23) Ahmed, T. S.; DeSimone, J. M.; Roberts, G. W. *Macromolecules* **2007**, *40* (26), 9322–9331.
(24) Ahmed, T. S.; DeSimone, J. M.; Roberts, G. W. *Macromolecules* **2008**, *41* (9), 3086–3097.
(25) Ameduri, B.; Boutevin, B. *J. Fluorine Chem.* **2000**, *104* (1), 53–62.
(26) Ameduri, B.; Boutevin, B.; Kostov, G. *Prog. Polym. Sci.* **2001**, *26* (1), 105–187.
(27) Combes, J. R.; Guan, Z.; DeSimone, J. M. *Macromolecules* **1994**, *27* (3), 865–867.
(28) DiNoia, T. P.; Conway, S. E.; Lim, J. S.; McHugh, M. A. *J. Polym. Sci., Part B: Polym. Phys.* **2000**, *38* (21), 2832–2840.
(29) Beuermann, S.; Imran-ul-Haq, M. *J. Polym. Sci., Part A: Polym. Chem.* **2007**, *45* (23), 5626–5635.
(30) Ahmed, T. S.; DeSimone, J. M.; Roberts, G. W. *Macromolecules* **2006**, *39* (1), 15–18.
(31) DeSimone, J.; Riddick, L. *Proc. NOBCChE* **1999**, *26*, 53–61.
(32) Mueller, P. A.; Storti, G.; Morbidelli, M.; Costa, I.; Galia, A.; Scialdone, O.; Filardo, G. *Macromolecules* **2006**, *39* (19), 6483–6488.
(33) Tai, H.; Liu, J.; Howdle, S. M. *Eur. Polym. J.* **2005**, *41* (11), 2544–2551.
(34) Tai, H.; Wang, W.; Howdle, S. M. *Macromolecules* **2005**, *38* (5), 1542–1545.
(35) Tai, H.; Wang, W.; Martin, R.; Liu, J.; Lester, E.; Licence, P.; Woods, H. M.; Howdle, S. M. *Macromolecules* **2005**, *38* (2), 355–363.
(36) Charpentier, P. A.; DeSimone, J. M.; Roberts, G. W. *Ind. Eng. Chem. Res.* **2000**, *39* (12), 4588–4596.
(37) Charpentier, P. A.; Kennedy, K. A.; DeSimone, J. M.; Roberts, G. W. *Macromolecules* **1999**, *32* (18), 5973–5975.
(38) Saraf, M. K.; Gerard, S.; Wojcinski, L. M.; Charpentier, P. A.; DeSimone, J. M.; Roberts, G. W. *Macromolecules* **2002**, *35* (21), 7976–7985.
(39) Beginn, U.; Najjar, R.; Ellmann, J.; Vinokur, R.; Martin, R.; Moeller, M. *J. Polym. Sci., Part A: Polym. Chem.* **2006**, *44* (3), 1299–1316.
(40) Tai, H.; Wang, W.; Howdle, S. M. *Macromolecules* **2005**, *38* (22), 9135–9142.
(41) Ahmed, T. S.; DeSimone, J. M.; Roberts, G. W. *Chem. Eng. Sci.* **2004**, *59* (22−23), 5139–5144.
(42) Charpentier, P. A.; DeSimone, J. M.; Roberts, G. W. *Chem. Eng. Sci.* **2000**, *55* (22), 5341–5349.
(43) Odian, G. *Principles of Polymerization*, 4th ed.; John Wiley & Sons: New York, 2004.
(44) Matyjaszewski, K.; Davis, T. P. *Handbook of Radical Polymerization*; Wiley-Interscience: New York, 2002.
(45) Ito, K.; O'Driscoll, K. F. *J. Polym. Sci., Polym. Chem. Ed.* **1979**, *17* (12), 3913–3921.
(46) Martin, R. Personal communication, Solvay Research and Technology Center, Brussels, Belgium, March 2008.
(47) Scanu, L. F.; DeSimone, J.; Roberts, G. W.; Khan, S. A. Abstracts of Papers, 229th ACS National Meeting, San Diego, CA, March 13−17, 2005 PMSE-376, 2005.
(48) Galia, A.; Cipollina, A.; Scialdone, O.; Filardo, G. *Macromolecules* **2008**, *41* (4), 1521–1530.
(49) Kennedy, K. A. Characterization of Phase Equilibrium Associated with Heterogeneous Polymerizations in Supercritcal Carbon Dioxide. Ph.D. Thesis, North Carolina State University, Raleigh, **2003**.
(50) Saraf, M. K. Polymerization of vinylidene fluoride in supercritical carbon dioxide: Molecular weight distribution. M.S. Thesis, North Carolina State University, Raleigh, **2001**.

MA801911J